PERGAMON

International Journal of Heat and Mass Transfer 44 (2001) 73–88

International Journal of
HEAT and MASS TRANSFER

www.elsevier.com/locate/ijhmt

Comparison of CHF measurements in R-134a cooled tubes and the water CHF look-up table

I.L. Pioro[a,*], D.C. Groeneveld[a,b], S.C. Cheng[a], S. Doerffer[b], A.Ž. Vasić[a], Yu. V. Antoshko[a]

[a]Department of Mechanical Engineering, University of Ottawa, Ottawa, Ont., Canada K1N 6N5
[b]Chalk River Laboratories, AECL Research, Chalk River, Ont., Canada K0J 1J0

Received 26 August 1999; received in revised form 26 February 2000

Abstract

An exhaustive experimental study of the critical heat flux (CHF) in R-134a-cooled tubes has been recently completed. The objective of this study was to provide a consistent set of CHF data to be used as a reference for future separate effect studies. The investigated range of flow parameters in R-134a was: outlet pressure 0.96–2.39 MPa (equivalent to 6–14 MPa in water), mass flux 500–3000 kg m^{-2} s^{-1} (equivalent to 700–4300 kg m^{-2} s^{-1} in water), and critical quality -0.1 to $+0.9$. To extend the range of critical qualities, different heated lengths (0.45–2 m) and two-phase flow at inlet to the test section were used. Scaling laws were applied to convert the standard CHF look-up table from water to R-134a equivalent conditions. The comparison of the data with the water-based look-up table showed that for high mass fluxes (G = 1400–4300 kg m^{-2} s^{-1} in water equivalent), the look-up table provides an excellent CHF prediction for R-134a-cooled tubes. The differences were mainly noticeable for the *limiting critical quality* range and for low mass flux. A discussion of the observed limiting critical quality phenomenon is also included.

1. Introduction

The original objective of this study was *to provide an exhaustive R-134a reference critical heat flux (CHF) database for vertical tubes covering a wide range of inlet and critical qualities*. This reference CHF database is required for comparison with R-134a data obtained in (i) non-circular geometries [1,2]; (ii) tubes containing various flow obstacles [3,4], and (iii) tubes positioned with various degrees of inclination from the vertical axis. The above separate effects studies have been performed in R-134a; the results will be applied to water-based systems, as previous papers have shown that refrigerants may be used with confidence to model CHF separate effects in water [5].

To assess the consistency of the CHF data trends, the R-134a data were also compared with corresponding CHF data sets obtained in water-cooled tubes. To permit such comparison, the water data must first be converted into refrigerant-equivalent values using fluid-to-fluid modeling relationships. Refrigerants such as R-12, R-22, R-134a have been used successfully in several heat transfer laboratories as modeling fluids for water [5–8]. It has been shown [6–8] that if the following fluid-to-fluid modeling relationships on which Katto's equations are based, are satisfied,

* Corresponding author. Tel.: +1-613-562-5800; fax: +1-613-562-5177.
E-mail address: ipioro@locutus.cc.uottawa.ca (I.L. Pioro).

0017-9310/01/$ - see front matter
PII: S0017-9310(00)00093-4

Nomenclature

D	inside diameter (mm)
D_{out}	outside diameter (mm)
$G=\rho u$	mass flux (kg m^{-2} s^{-1})
H	enthalpy (J kg^{-1})
h_{fg}	latent heat of vaporization (J kg^{-1})
L	heated length (m)
L_t	total length (m)
p	pressure (MPa)
q	heat flux (kW m^{-2})
T	temperature (°C)
u	velocity (m s^{-1})
x_{in}	inlet vapor quality
x_{cr}	critical vapor quality
x_{cr}^{lim}	limiting critical quality

Greek symbols

Δ	difference
δ	thickness (mm)
ρ	density (kg m^{-3})
σ	surface tension (N m^{-1})

Subscripts

cr	critical
exp	experimental
f	liquid
g	vapor
in	inlet
pred	predicted
R	R-134a
W	Water
w	wall

Abbreviations

AECL	Atomic Energy of Canada Limited
CHF	critical heat flux
DC	direct current
ID	inside diameter
NSERC	Natural Sciences and Engineering Research Council of Canada
RMS	root mean square

- $L_R = L_W$, $D_R = D_W$ (geometric similarity),
- $\left[\frac{G}{\left(\frac{\rho_f\sigma}{D}\right)^{0.5}}\right]_R = \left[\frac{G}{\left(\frac{\rho_f\sigma}{D}\right)^{0.5}}\right]_W$ and $(\frac{\rho_f}{\rho_g})_R = (\frac{\rho_f}{\rho_g})_W$ (hydrodynamic similarity),
- $x_{cr\,R} = x_{cr\,W}$ (thermodynamic similarity).

then the dimensionless CHF is expressed as

$$\left[\frac{q_{cr}}{Gh_{fg}}\right]_R = \left[\frac{q_{cr}}{Gh_{fg}}\right]_W$$

will also be the same for both fluids (note subscript R referred to refrigerant and subscript W to water), D is in m, and q is in W m^{-2}.

Rather than randomly selecting a water-CHF data set (from the many data sets available) for comparison with the R-134a data, it was decided to use the CHF look-up table [9] as this represents an already normalized CHF database for water. The table was thus converted into equivalent R-134a conditions using the above relationships and its CHF values were subsequently compared with the R-134a values. The comparison showed generally surprisingly good results; hence, the present investigation was expanded to include the following important second objective *to assess the suitability of the reference CHF look-up table for water for predicting the R-134a CHF data*. An earlier study [7] examined the suitability of a preliminary version of the look-up table and also found it very promising in modeling (or *scaling*) the CHF of seven different fluids, although the range of qualities covered at that time in these fluids was much more limited.

2. CHF look-up table approach

CHF under flow boiling has been thoroughly investigated for circular tubes and many CHF prediction methods have been proposed. However, no single correlation or model has been found capable of predicting the CHF over a wide range of flow parameters, because of the complexity of the boiling crisis mechanism. Recently, a very promising methodology, the CHF look-up table [9], has been developed, which has a much wider range of validity. The look-up table approach is based on the assumption that the CHF for an 8 mm ID vertical tube is only a function of pressure, mass flux, and critical quality. For tube diameters different from 8 mm, a simple correction can be applied based on Eq. (1):

$$\frac{\mathrm{CHF}_D}{\mathrm{CHF}_{D=8\ \mathrm{mm}}} = \left(\frac{D}{8}\right)^n, \tag{1}$$

where D is inside diameter of a circular tube in mm, $D = 8$ mm is the inside diameter of a reference circular tube from the look-up table, and n is an exponent. This relationship is valid for a constant value of critical quality, and n is assumed constant independent of the diameter value for a wide range of diameters. Although a range of values for n have been proposed, the commonly accepted value of n is -0.5 [9–11]. The CHF vs. x_{cr} relationship eliminates the need for a heated length's dependence. The effect of a heated length becomes important only for short tubes with $\frac{L}{D} < 50$.

3. Experiments

3.1. General

The experimental study was performed in the University of Ottawa's multi-fluid loop using R-134a as a coolant. The loop has been described in previous papers [1,2] and only a brief summary is provided in the following section. The main difference with the pre-

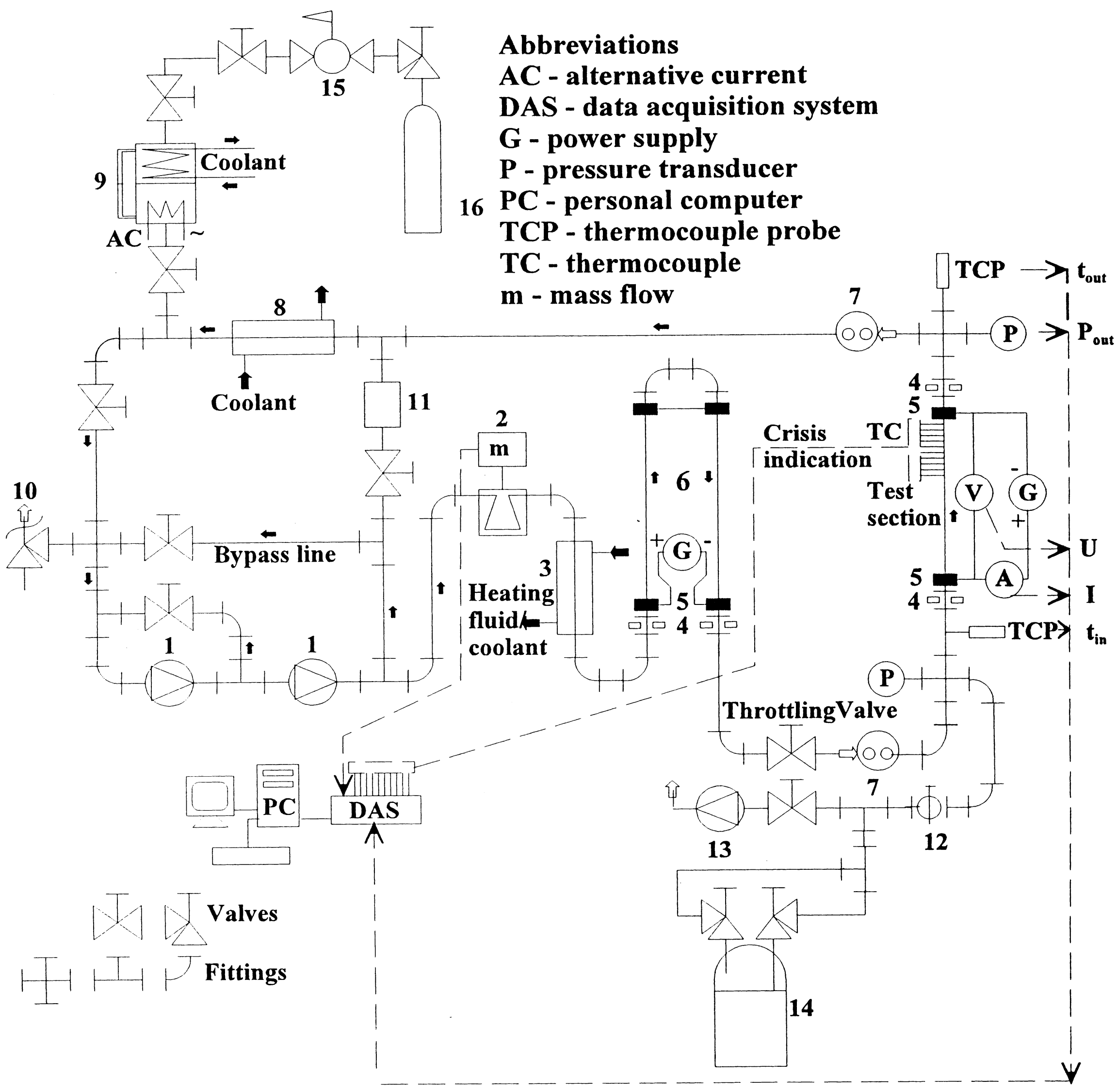

Fig. 1. Experimental multi-fluid loop. 1: gear pump, 2: Coriolis type mass flow meter, 3: preheater, 4: dielectric fittings, 5: electric power terminals, 6: electrical preheater, 7: sight glass, 8: condenser, 9: pressurizer, 10: pressure relief valve, 11: refrigerant filter-drier, 12: ball valve, 13: vacuum pump, 14: refrigerant storage tank, 15: pressure reducer, 16: nitrogen container.

vious tests is the use of a two-phase flow inlet which required a heat balance across the preheater.

3.2. Experimental equipment

The multifluid loop (Fig. 1) was designed and built at the Department of Mechanical Engineering, University of Ottawa. It has been used previously for CHF and post-CHF tests with R-12, R-22, R-113, and R-134a. The main components of the loop are: test section (Table 1), condenser (heat exchanger with cold water), pressurizer with electrical heater and coils for cold water, preheater (inverted U-tube ID 9.7 mm, L = 3.4 m, which was electrically (Joule) heated) and a heat exchanger with hot/cold water, two pumps (connected in series), and power supplies for the test section (DC, maximum 40 V × 300 A) and for the preheater (DC, maximum 40 V × 150 A), and related instrumentation (flow-meter, thermocouples, data acquisition system, voltmeter, ammeter, pressure transducer with sensor, etc.).

Great care was taken to avoid pressure pulsations during experiments, especially at low flows. For this purpose, the hydraulic resistance for two-phase flow from the test section outlet and to the inlet of the condenser was reduced by eliminating any valves and sharp turns for flow with smooth bending of the tubes or through high-pressure flexible hoses. Also, a throttling valve was installed at the inlet of the test section to ensure high hydrodynamic stability of the flow inside the experimental loop. For the experiments with two-phase flow at inlet, the throttling valve was installed just upstream of the preheater. Several sight-glasses were used to detect the onset of boiling.

3.3. Test sections

The test section was oriented vertically with upward flow and was resistance heated via a large DC current passing through the wall. Two test sections were used during these tests (Table 1). The heated length was varied to provide maximum variation in critical quality. To detect dryout, 12 fast response K-type thermocouples with self-adhesive backing were used. These thermocouples allowed to record small changes in a wall temperature and were flexible enough to be installed on rounded surfaces.

Two copper power terminals were installed on the test section. The major series of experiments were carried out at saturation conditions with single-phase fluid at inlet.

3.4. Test procedure

Before each series of experiments, a heat balance test was performed. Also, periodically the *Quality Assurance* points (the *QA* points conditions for several heated lengths were: $p = 1.67$ MPa, $G = 2000$ kg m^{-2} s^{-1}, and inlet temperature 30°C) were obtained. The comparison of the CHF values of QA points for particular heated length during several years did not uncover any significant differences (for $L = 0.45$ m, the deviation from the CHF arithmetic average value is not more than $\pm 2\%$, and for $L = 1$ and 2 m, deviation is less than $\pm 1\%$).

Just prior to CHF occurrence, all test conditions were stabilized and the power to the test section was raised in small steps. CHF was defined as the first detected occurrence of a wall temperature excursion just below the upper power terminal. At that moment, all values of the parameters were recorded and the power to the test section was decreased. In general, after that, a new value of inlet temperature was set-up. Usually, the value of inlet temperature increment was about 2–3°C. Once the complete range in inlet temperatures had been covered, the mass flux was changed to the next value of the test matrix. After that, the same procedure was repeated for the different heated lengths, and later on, a value of the outlet pressure was set-up according to the test matrix.

To extend the range of critical quality to higher values, it was decided to use two-phase flow at the test section inlet, especially for the maximum heated length

Table 1
Test sections dimensions

D (mm)	D_{out} (mm)	δ_w (mm)	L_t (m)	L (m)	Material
6.92	7.94	0.51	2.1	0.45–2	Inconel 600
4.67	6.35	0.84	1.34	0.45–1.3	Inconel 601

Table 2
Test matrix conditions in R-134a and their water-equivalent conditions

p_R (MPa)	p_W (MPa)	G_R (kg m^{-2} s^{-1})			
		500	1000	2000	3000
		G_W (kg m^{-2} s^{-1})			
0.96	6	714	1427	2855	4282
1.13	7	712	1423	2847	4270
1.31	8	711	1423	2846	4269
1.67	10	707	1415	2830	4245
2.03	12	699	1398	2879	4194
2.39	14	702	1403	2806	4209

of 2 m. Two-phase flow was generated in the electrical preheater by means of resistance heating. The outlet quality for the preheater was calculated and this value was used as the inlet quality for the test section. To check that two-phase flow at inlet of the test section does not introduce additional significant uncertainties on the CHF measurements, usually several points were obtained with single-phase fluid at the inlet, after which, with power increasing in the preheater, two-phase flow was obtained.

3.5. Test matrix

The following test conditions were covered in the present investigation: test section outlet pressure 0.96, 1.13, 1.31, 1.67, 2.03, and 2.39 MPa, mass flux 500, 1000, 2000, and 3000 kg m^{-2} s^{-1}, and inlet temperature ranged from minimum temperature to a saturated one. The minimum inlet temperatures depended on the cooling water temperatures and varied from 3°C in winter to 22°C in summer. The equivalent water-based conditions are shown in Table 2.

3.6. Experimental errors

Heat balance tests showed that the heat losses were not more than 1–2% (in absolute values not more than 20 W for the test section, and 50 W for the preheater) of total power input. CHF measurement errors were not more than 2.5% (4.5% for the experiments with two-phase flow at inlet). Errors for measuring mass flux and pressure were not more than 0.3 and 1%, respectively. The temperatures were measured with an accuracy better than ±0.5°C.

4. Test results

4.1. General

The tests results are presented graphically in three ways:

- As is a common practice and to facilitate comparison with the look-up table, the results were first presented on a CHF vs. critical quality basis. This permits a combination of all data obtained for a given pressure and mass flux irrespective of heated length (which varied from 0.45 to 2 m) or two-phase flow inlet.
- In addition, for some cases, the data were presented in the form of CHF vs. inlet quality for each heated length. The predictions of the look-up table are also shown. They were produced by finding the intersection between the CHF vs. x_{cr} relationship of the look-up table and the heat balance line

$$x_{cr} = \frac{4q_{cr}L}{GDh_{fg}} - x_{in}, \tag{2}$$

where q_{cr} is in W m^{-2}, D is in m, and $x_{in} = \frac{\Delta H_{in}}{h_{fg}}$, and applying the correction for the diameter difference from the reference 8 mm value of the table.

- Finally, some of the CHF vs. x_{in} data were normalized to the equivalent heated length of 1.98 m. This permitted a combination of all the heated lengths and of the two-phase flow inlet data. The latter comparison provided an extra check on the consistency of the data as, in general, the CHF vs. x_{in} plots show a linear trend for x_{in} < 0. The conver-

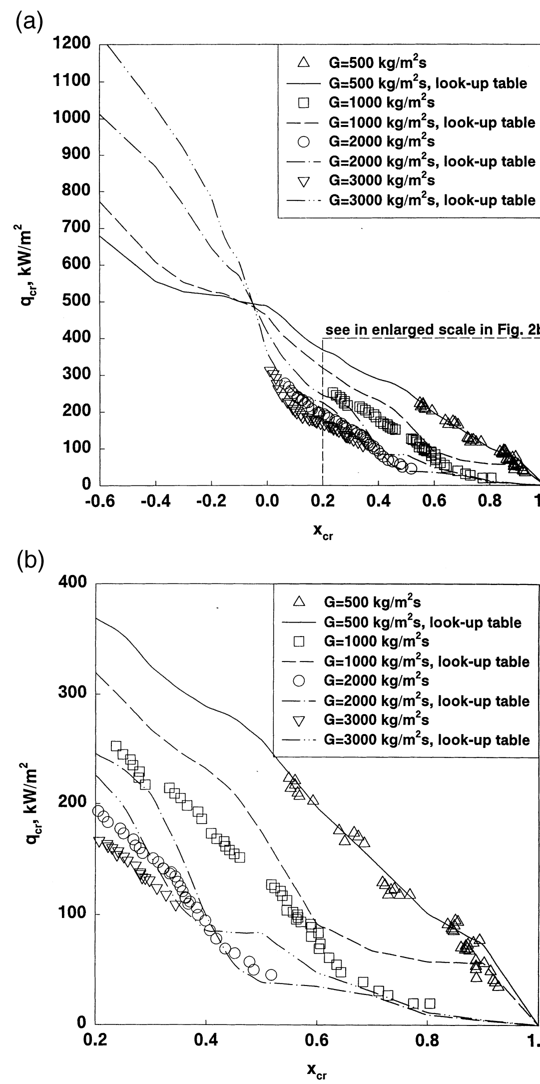

Fig. 2. Effect of critical quality on CHF in circular tube at different mass fluxes: (a) R-134a, $p = 0.96$ MPa, $D = 6.92$ mm, $L = 0.45$–1.98 m; (b) same in enlarged scale.

sion to the equivalent heated length uses an adjustment which adds an extra heated length (ΔL) to the shorter tubes and lowers the inlet enthalpy by $\Delta H'_{\rm in}$ such that the heat balance across the added heated ΔL is satisfied, i.e., $\Delta H'_{\rm in} = \frac{4q_{\rm cr}\Delta L}{GD}$, where q is in W m^{-2} and D is in m.

The CHF vs. $x_{\rm in}$ plots are also useful in assessing the accuracy of the look-up table prediction.

For this particular purpose, data from the look-up table were converted into inlet quality conditions as follows: (1) through scaling law the data were converted from water to R-134a critical quality conditions, (2) then the correction for D according to Eq. (1) was applied, (3) after that through the modified Eq. (2) the value of inlet quality was determined based on the same heated length as the present experimental data.

Note that all the figures only show the data obtained in a 6.92 mm ID tube as our primary experimental data, other diameters data have been converted to this diameter.

4.2. CHF vs. $x_{\rm cr}$ presentation

Figs. 2–7 show the CHF vs. $x_{\rm cr}$ graphs for the four primary flows ($G = 500$, 1000, 2000, and 3000 kg m^{-2} s^{-1}) and pressures of 0.96, 1.13, 1.67, 2.03, and 2.39

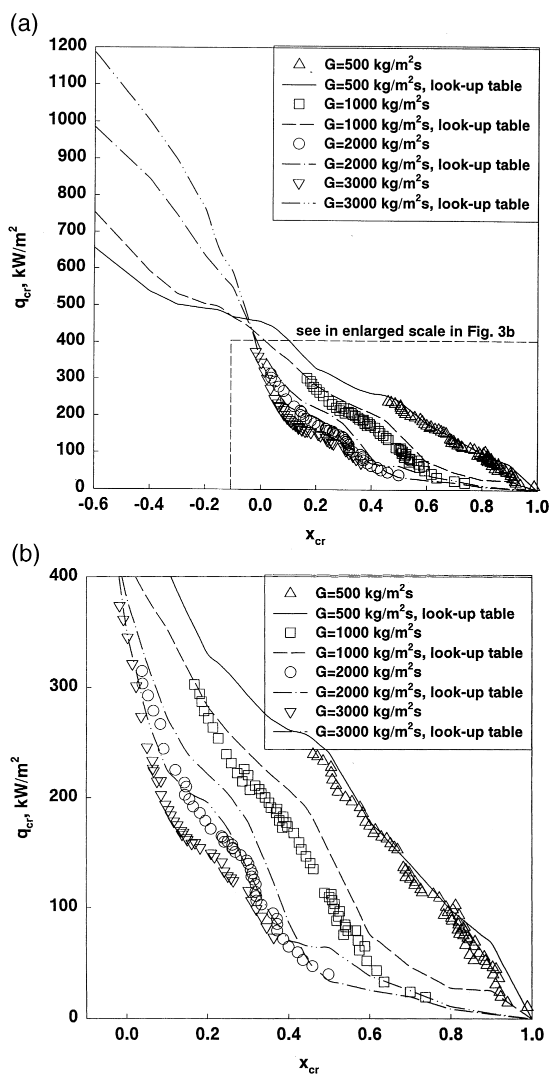

Fig. 3. Effect of critical quality on CHF in circular tube at different mass fluxes: (a) R-134a, $p = 1.13$ MPa, $D = 6.92$ mm, $L = 0.45$–1.98 m; (b) same in enlarged scale.

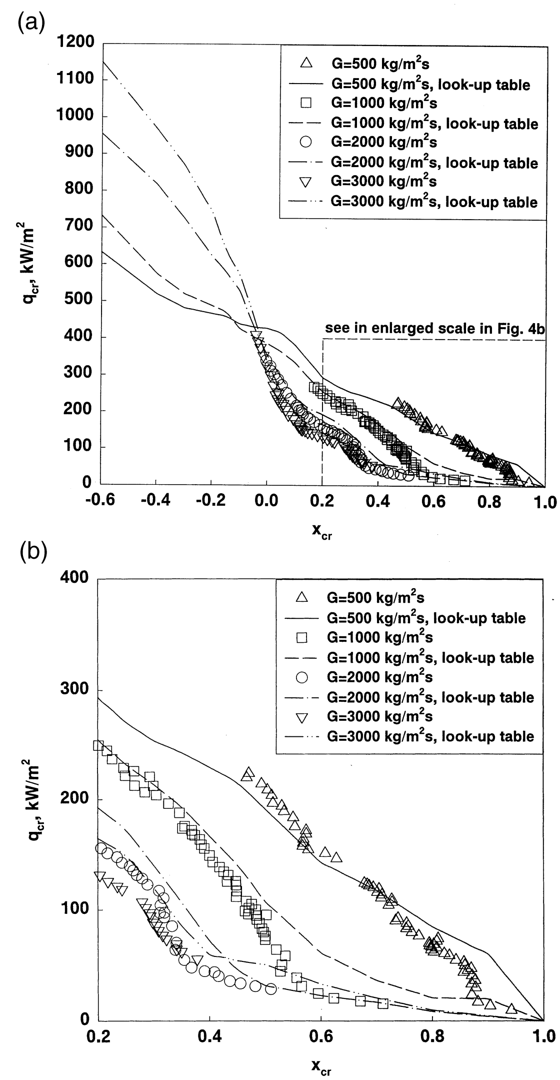

Fig. 4. Effect of critical quality on CHF in circular tube at different mass fluxes: (a) R-134a, $p = 1.31$ MPa, $D = 6.92$ mm, $L = 0.45$–1.98 m; (b) same in enlarged scale.

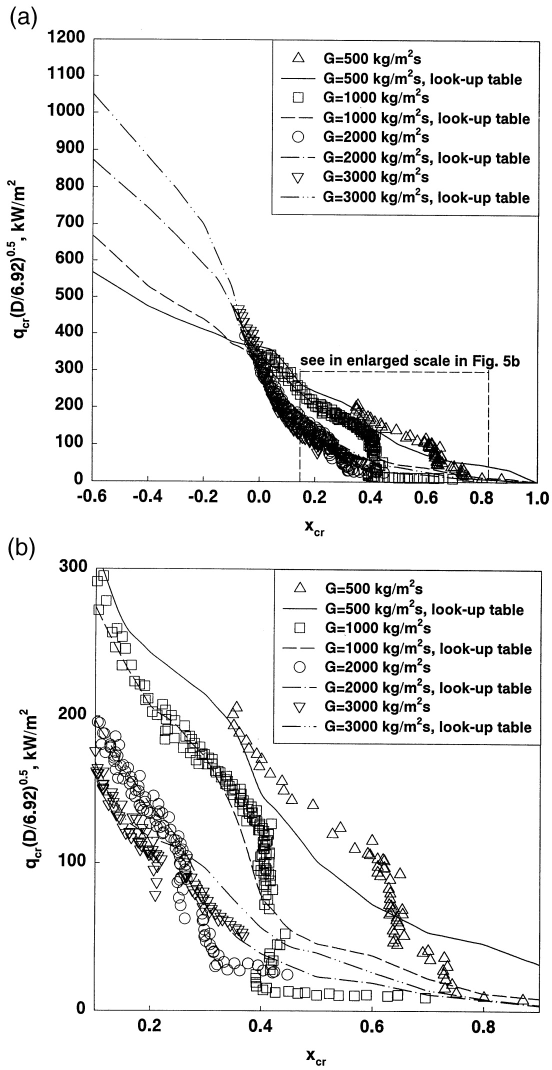

Fig. 5. Effect of critical quality on CHF in circular tube at different mass fluxes: (a) R-134a, $p = 1.67$ MPa, $D = 4.67$ and 6.92 mm, $L = 0.45$–1.98 m; (b) same in enlarged scale.

MPa. In each plot, the R-134a-equivalent prediction of the look-up table for a 6.92 mm ID tube is also shown. The following observations can be made:

- The data generally follow the look-up table predictions closely, except at critical qualities near and above the limiting quality range.
- A limiting critical quality (for details, see Section 5.1) is clearly present at $p = 1.67$, 2.03, and 2.39 MPa (Figs. 5–7) but it appears less pronounced or disappears altogether at the lower pressures (Figs. 2–4).
- The "inverse mass flux effects" [12], where all CHF vs. x_{cr} curves cross such that at higher qualities, the CHF decreases with an increase in mass flux, are clearly present for all pressures. Although the data do not always cover the complete range of critical qualities, their trend is nevertheless in agreement with the look-up table.

Some of the above trends can be seen more clearly in Figs. 2b–7b where the scales are enlarged. Also, in these figures, the additional or local cross-over points of CHF vs. x_{cr} curves can be seen for several mass flux values and this appears to be due to different CHF drops at the limiting critical quality range (Figs.

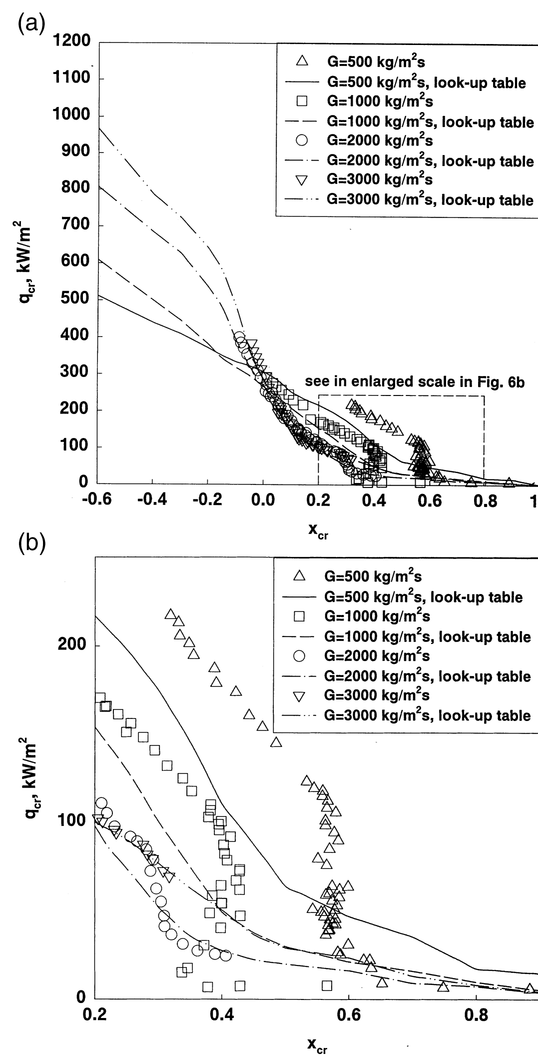

Fig. 6. Effect of critical quality on CHF in circular tube at different mass fluxes: (a) R-134a, $p = 2.03$ MPa, $D = 6.92$ mm, $L = 0.45$–1.98 m; (b) same in enlarged scale.

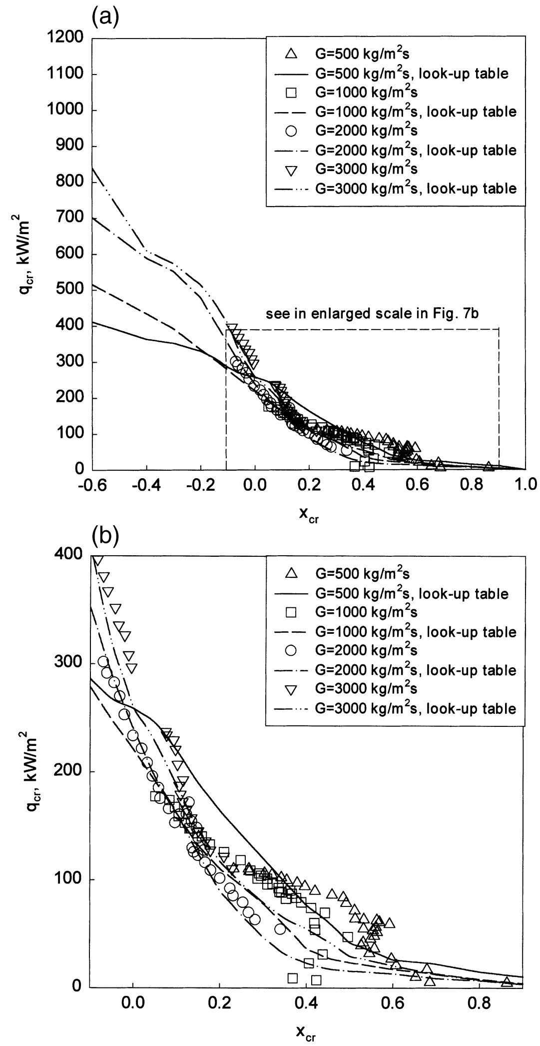

Fig. 7. Effect of critical quality on CHF in circular tube at different mass fluxes: (a) R-134a, $p = 2.39$ MPa, $D = 6.92$ mm, $L = 0.45$–1.98 m; (b) same in enlarged scale.

5b, 6b, and 7b). The look-up table also shows such trends but not for all flows.

Figs. 8–11 show the effect of heated length and two-phase flow inlet for $p = 1.67$ MPa and $G = 500$, 1000, 2000, and 3000 kg m^{-2} s^{-1}. The results do not display a significant effect of heated length or two-phase flow inlet on the CHF. It is clearly shown in Fig. 10b, where the two-phase flow inlet data obtained in a shorter heated length (0.45 m) are present. When the single- and two-phase flow inlet results were analyzed using an identical methodology (based on the pre-heater inlet temperature), no differences between single- and two-phase flow inlet could be detected.

4.3. CHF vs. x_{in} presentation

Figs. 12 and 13 present the CHF results as a function of inlet quality, either for different heated lengths (Fig. 12) or for the normalized heated length (Fig. 13, where the results for four flows all heated lengths and two-phase flow inlets are combined in one figure). These figures show that:

- A linear relationship between CHF and x_{in} clearly exists over a wide range of qualities; only at positive inlet qualities does a deviation in the linear relationship become evident; this deviation is not due to the presence of a two-phase flow inlet but rather due to the fact that the CHF would have become negative at x_{in} between 0.4 and 0.6, if the linearity would have continued (Fig. 12). The correct asymptotic trend as displayed by the look-up table results in $q_{cr} = 0$ for $x_{in} = 1.0$.
- No effect of the heated length can be observed in Fig. 13, hence, the normalizing procedure as described in Section 4.1 correctly accounts for the heated length effect.
- The agreement between the look-up table and our experimental data is even better on a CHF vs. x_{in} basis than on a CHF vs. x_{cr} basis. This was also discussed by Groeneveld et al. [5] previously. Only at very low CHF values for $x_{cr} > x_{cr}^{lim}$ does the error become noticeable. In all cases, the deviation from the look-up table is much smaller for the CHF at constant x_{in} than for the CHF at constant x_{cr} (Fig. 5b). Note that the error based on a constant x_{in} should be quoted as in any experiment x_{in} is an independent parameter set by the inlet temperature or inlet enthalpy, while x_{cr} is not known prior to a CHF measurement but is a function of CHF.
- Although the CHF vs. x_{cr} plot clearly shows the

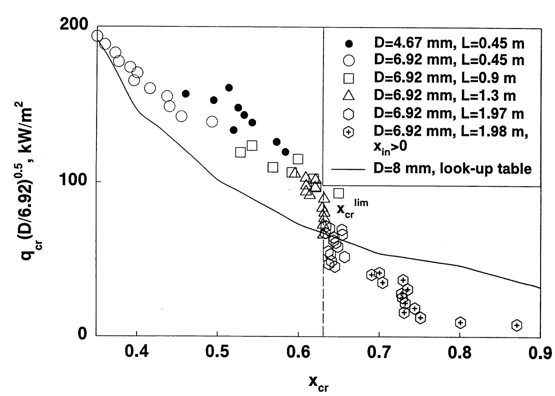

Fig. 8. Effect of critical quality on CHF in circular tube: R-134a, $p = 1.67$ MPa, $G = 500$ kg m^{-2} s^{-1}.

presence of a limiting critical quality in Figs. 5–7, this effect is rather difficult to see in Figs. 12 and 13.

4.4. Effect of pressure

Fig. 14 summarizes the effect of pressure on a CHF vs. x_{cr} plot, while Fig. 15 shows the same on a CHF vs. x_{in} plot. The results again show a much less scatter and better agreement with the look-up table on a CHF vs. x_{in} plot than on a CHF vs. x_{cr} plot. A close examination of Fig. 14 shows that the limiting critical quality switches to a lower quality with an increase in pressure.

5. Discussion

5.1. Limiting critical quality phenomenon

Some disagreement exists in the literature whether the *limiting critical quality* really exists. This term orig-

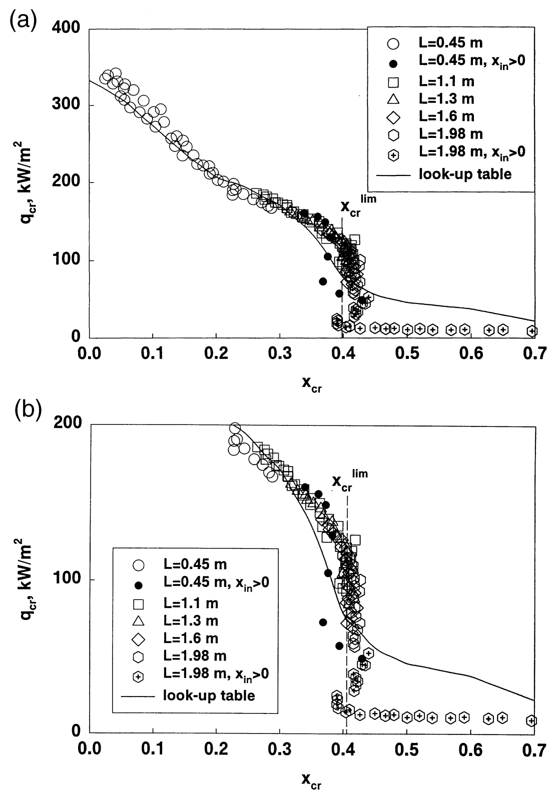

Fig. 9. Effect of critical quality on CHF in circular tube ($D = 6.92$ mm): (a) R-134a, $p = 1.67$ MPa, $G = 1000$ kg m^{-2} s^{-1}; (b) same in enlarged scale.

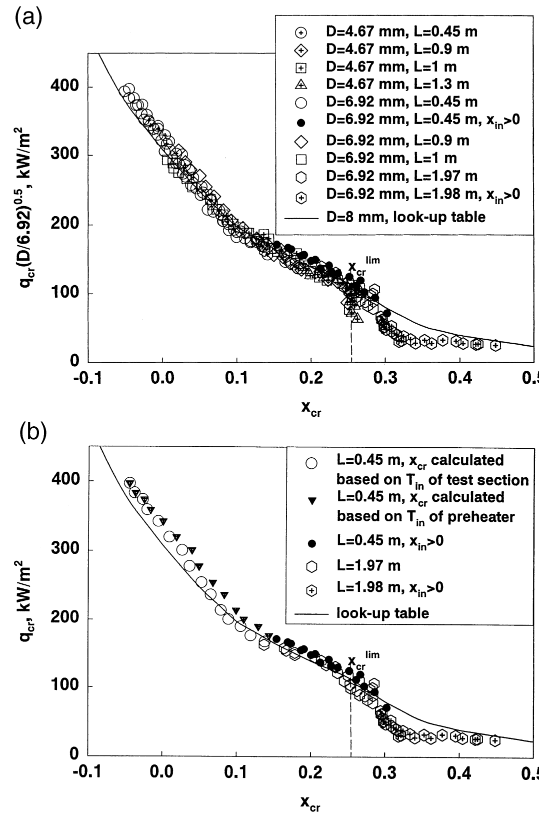

Fig. 10. Effect of critical quality on CHF in circular tube: (a) R-134a, $p = 1.67$ MPa, $G = 2000$ kg m^{-2} s^{-1}; (b) R-134a, $p = 1.67$ MPa, $G = 2000$ kg m^{-2} s^{-1}, $D = 6.92$ mm (comparison of two different methods of x_{cr} evaluation based on the test section inlet temperature (standard method for single-phase flow inlet) and based on the inlet temperature to the preheater (standard method for two-phase flow at test section inlet).

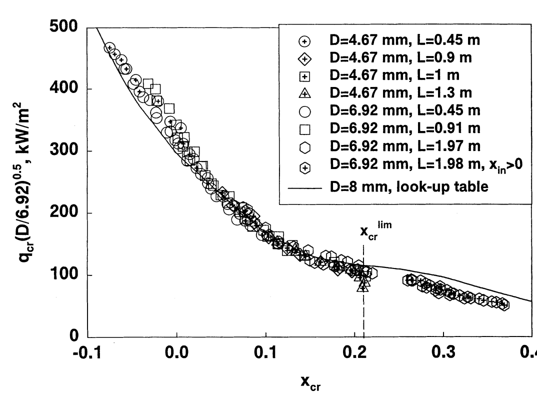

Fig. 11. Effect of critical quality on CHF in circular tube: R-134a, $p = 1.67$ MPa, $G = 3000$ kg m^{-2} s^{-1}.

inated in the Russian literature [10,11,13–15] and the evidence for the existence of this phenomenon, as observed in water CHF tests, was reviewed by Kitto [16]. It may be better to refer to this phenomenon as a sharp change in slope on the CHF vs. x_{cr} plot. This change in slope can be very dramatic and appears to correspond to a *limiting critical quality* for certain conditions. The sharp change in slope is probably caused by a change in CHF mechanism in the annular flow regime, from the so-called *entrainment-controlled dryout* (typical for the lower qualities where the liquid film is fairly thick and is being depleted by a combination of entrainment and evaporation while being replenished by deposition), to a *deposition-controlled dryout* (where the liquid film is too thin to permit significant entrainment,and where the film dryout can only be prevented by significant deposition [17]). This change in slope can be predicted analytically using Hewitts annular flow model [17]. As can be seen in Figs. 5b, 6b, 7b–9, during this change in CHF mechanism, there can be a very large drop in CHF over a very narrow range of quality. This agrees with observations by Levitan and Lantsman [14], who observed a CHF drop up to 10 times in water at a virtually constant value of the critical quality.

An examination of Figs. 2–7 and 14 suggests that the limiting critical quality was observed to be more pronounced for the higher pressures and lower mass velocities. It appears that the limiting quality shifts to lower quality with an increase in pressure and mass flux. This general trend agrees with the observations of others (e.g., see review by Kitto [16]). Doroschuk et al. [10] published a table of limiting critical quality values for water as a function of pressure and flow. If we interpret the change in slope on the CHF vs. x_{cr} plot as a *limiting critical quality* then this table of values is in reasonable agreement with our water-equivalent data (see [18]). In general, the equations recommended by Doroschuk et al. [10] and our previous data [18] show an increase in x_{cr}^{lim} with an increase in diameter.

It is interesting to note that while the CHF vs. x_{cr} graphs show at times a very dramatic limiting critical quality presence, the CHF vs. x_{in} graphs (e.g., Figs. 12, 13, and 15) hardly show any perturbation at all.

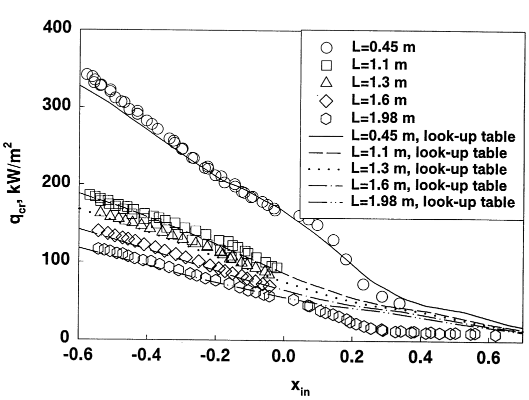

Fig. 12. Effect of inlet quality on CHF in circular tube: R-134a, $p = 1.67$ MPa, $G = 1000$ kg m^{-2} s^{-1}, $D = 6.92$ mm.

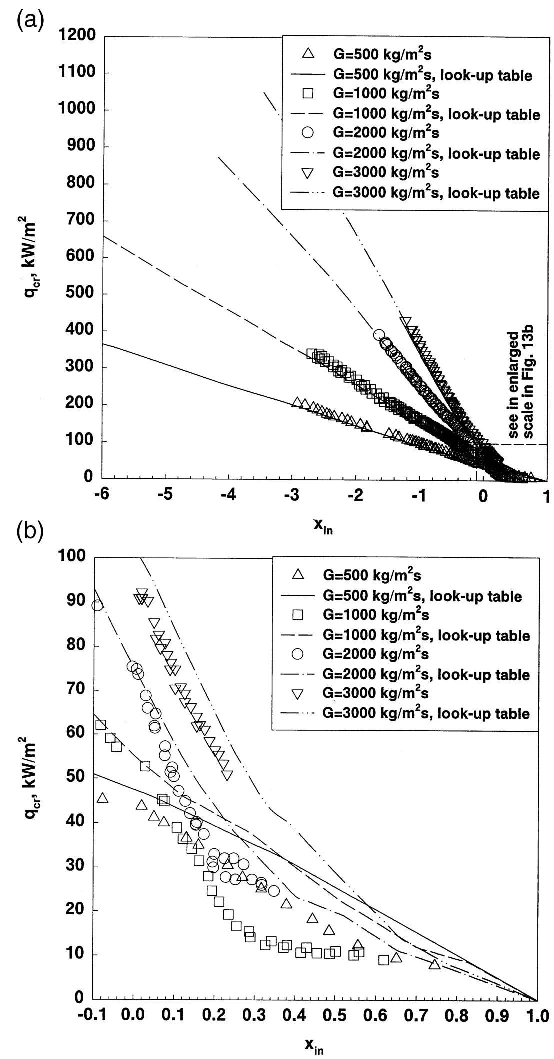

Fig. 13. Effect of inlet quality on CHF in circular tube at different mass fluxes: (a) R-134a, $p = 1.67$ MPa, $D = 6.92$ mm; data for tubes $L = 0.45$, 0.9, 1, 1.3 and 1.6 m converted to heated length 1.98 m; look-up table, $L = 1.98$ m; (b) same in enlarged scale.

5.2. Comparison of the data with the CHF look-up table

All individual R-134a CHF results were compared to the predictions of the look-up table (after applying the aforementioned conversions to obtain R-134a equivalent values for a 6.94 mm ID tube). All predictions were made based on known inlet conditions (the so-called *Heat Balance Method*, or *HBM*, see also discussion by Heljzar and Todreas [19]) rather than the dependent critical quality parameter. The deviations from the look-up table are shown graphically in Appendix A. The following conclusions may be drawn:

- The error histogram shows that 81% of all 1031 data points have prediction errors less than ±10% and 93% with errors less than ±20%. For the 806 single-phase inlet data points, 90% of the data were predicted with errors less than ±10% and 99% with errors less than ±20%.
- The largest deviation from the look-up table were observed with the data obtained with positive inlet qualities. Here we see much greater deviations.

Note that these high deviation error data points correspond to the data obtained almost exclusively at $x_{cr} \geq x_{cr}^{lim}$. The following reasons for these larger discrepancies have been identified:

- CHF measurements with two-phase flow inlet have a higher uncertainty in critical quality, due to the evaluation of the enthalpy rise across the preheater and extra heat losses from the piping between the preheater and the test section.
- The R-134a CHF data trends in high error region are different from that of the look-up table, with the CHF look-up table showing a more gradual variation in CHF. This difference may be due to: (i) the look-up table database contained no two-phase flow inlet data and, as a result, very few data in the database were obtained at $x_{cr} \geq x_{cr}^{lim}$ (as this would have required very long test sections), (ii) the CHF vs. x_{cr} relationship of the look-up table has undergone a

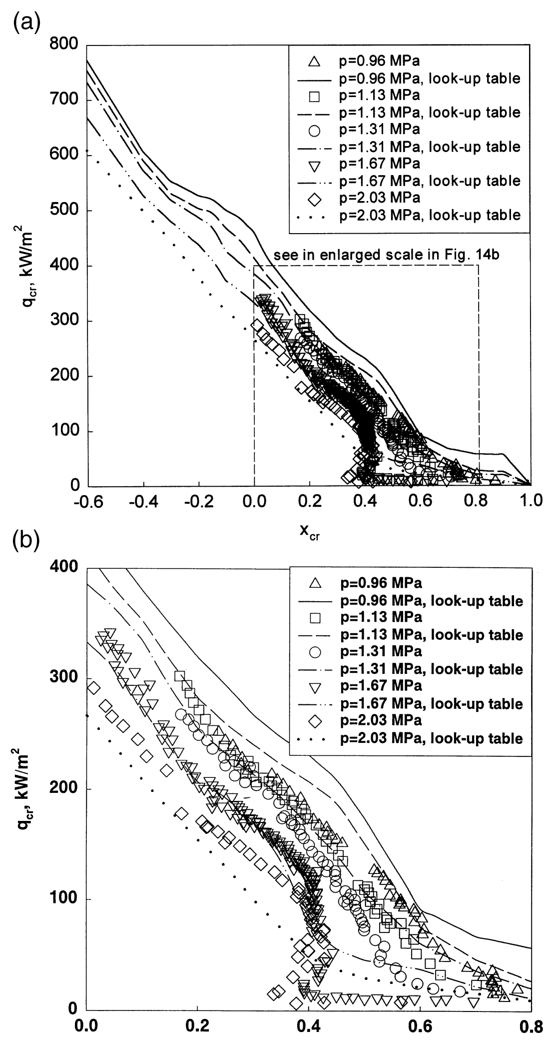

Fig. 14. Effect of critical quality on CHF in circular tubes at different pressures: (a) R-134a, $G = 1000$ kg m^{-2} s^{-1}, $D = 6.92$ mm, $L = 0.45$–1.98 m; (b) same in enlarged scale.

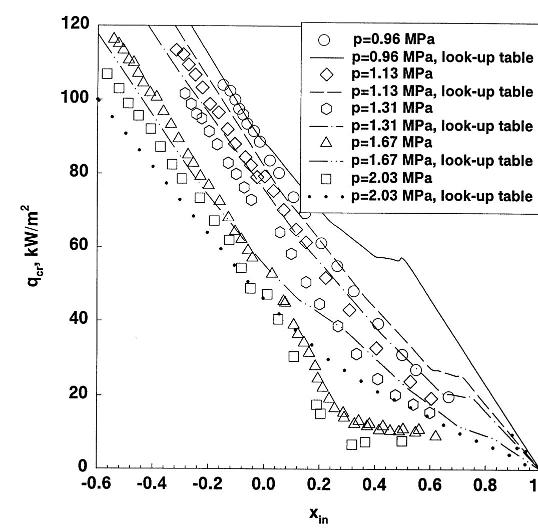

Fig. 15. Effect of inlet quality on CHF in circular tubes at different pressures: R-134a, $G = 1000$ kg m^{-2} s^{-1}, $D = 6.92$ mm, $L = 1.98$ m.

smoothing operation to remove any small discontinuities, and (iii) the limiting quality region is not well understood and varies with tube diameter.

- Those CHF values with large discrepancy errors also had a very low CHF value (e.g., see Figs. 2b–6b), where CHF values were only a fraction of the CHF values observed at pre-limiting quality conditions. Hence, uncertainties due to heat losses and in the evaluation of two-phase flow inlet became much more important.

A comparison of Figs. 5, 8–11 and 14, and Figs. 12, 13, and 15 suggests that while the local conditions plots show a more significant scatter and non-linearities, these perturbations almost disappear in the CHF vs. x_{in} plots and, hence, are not due to heated length or two-phase flow inlet effects. Since the critical quality is a calculated value which depends on the actual measured CHF value, any small variation on a CHF vs. x_{in} plot is always magnified considerably on a CHF vs. x_{cr} plot. This degree of magnification depends on the slope of the CHF vs. x_{cr} curve and varies from no amplification for a horizontal line to an almost infinite amplification for a vertical line, such as for a true limiting quality case.

Figs. 8–13 also demonstrate that there was no observable effect of two-phase flow inlet or heated length on CHF, thus negating the argument discussed by Kitto [16] that the limiting quality observation is due to the presence of two-phase flow inlet.

Despite the above limitations, it is encouraging to note that a CHF prediction method (the look-up table) which is based solely on water data, can be used with considerable success in predicting the refrigerant data.

6. Conclusions and final remarks

1. CHF experiments were performed in circular tubes in R-134a covered a wide range of pressures and mass velocities. To provide as wide range of critical qualities as possible, various heated lengths were used and extensive testing with two-phase flow inlet was performed.
2. The results were compared with predictions from the CHF look-up table after applying the fluid-to-fluid modeling laws and applying a standard correction for the diameter difference.
3. The agreement between the CHF look-up table [9] and the experiment is surprisingly good. Only at qualities near the so-called *limiting critical quality region* (the region where the CHF drops of vary rapidly with increasing inlet quality) do we see a different trend, with the look-up table showing a more gradual variation in CHF. This difference may be due to the fact that the CHF vs. x_{cr} relationship of the look-up table has undergone a smoothing operation to remove any small discontinuities.
4. The limiting critical quality was observed to be more pronounced for the higher pressures and lower mass fluxes. The limiting quality shifts to a lower quality with an increase in pressure and mass flux. On a water-equivalent basis, the observed trends in limiting critical quality are in good agreement with previously reported values for water-cooled tubes.

Acknowledgements

The financial support provided by AECL and NSERC is gratefully acknowledged.

Appendix A. Assessment of prediction errors with respect to water-based CHF look-up table

The CHF look-up table was converted to R-134a equivalent conditions and corrected for the diameter effect using Eq. (1) with $n = -0.5$. The R-134a version of the look-up table was then compared to the University of Ottawa R-134a CHF data (1031 points) and the results are shown in Fig. A1a–f). The largest prediction errors corresponded to the very low CHF data, which were obtained at critical qualities near or above the limiting quality; to get these high qualities usually requires the use of two-phase flow inlet conditions. The average prediction error and RMS prediction error for all 1031 data points were 7 and 23%, respectively. For the 806 single-phase inlet data points, these prediction errors were 0.5 and 10%. Reasons for the high prediction errors with the two-phase flow inlet data were already discussed in Section 5.2.

The prediction errors were evaluated using the following definitions:

$$\text{Error} = \frac{\text{Value}_{\text{pred}} - \text{Value}_{\text{exp}}}{\text{Value}_{\text{exp}}},$$

$$\text{Mean Error} = \frac{1}{n}\sum_{i=1}^{i=n}\text{Error}_i,$$

$$\text{RMS Error} = \sqrt{\frac{1}{n}\sum_{i=1}^{i=n}\text{Error}_i^2}.$$

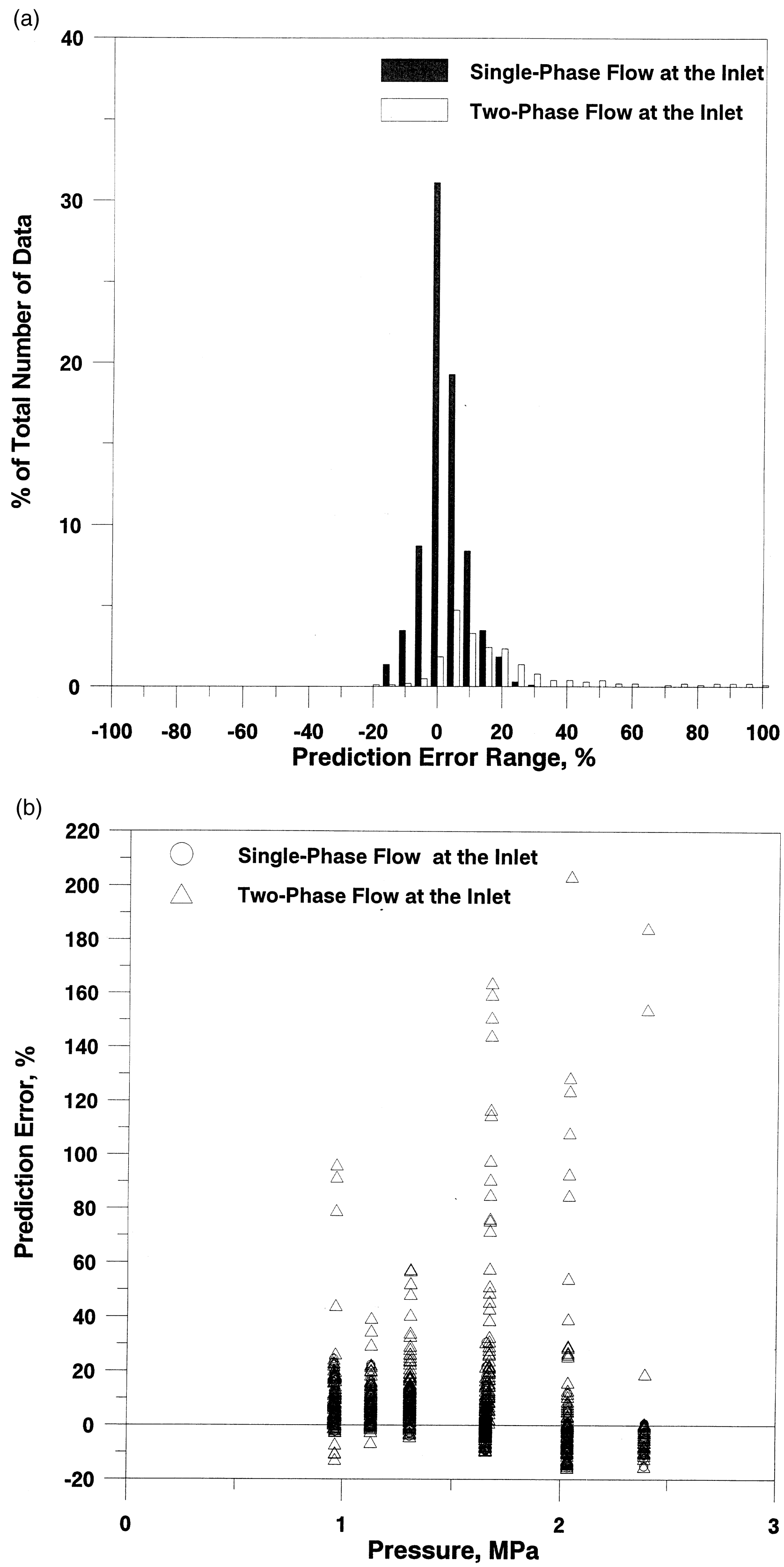

Fig. A1. Comparison of the University of Ottawa R-134a CHF data over water-based CHF look-up table prediction [9].

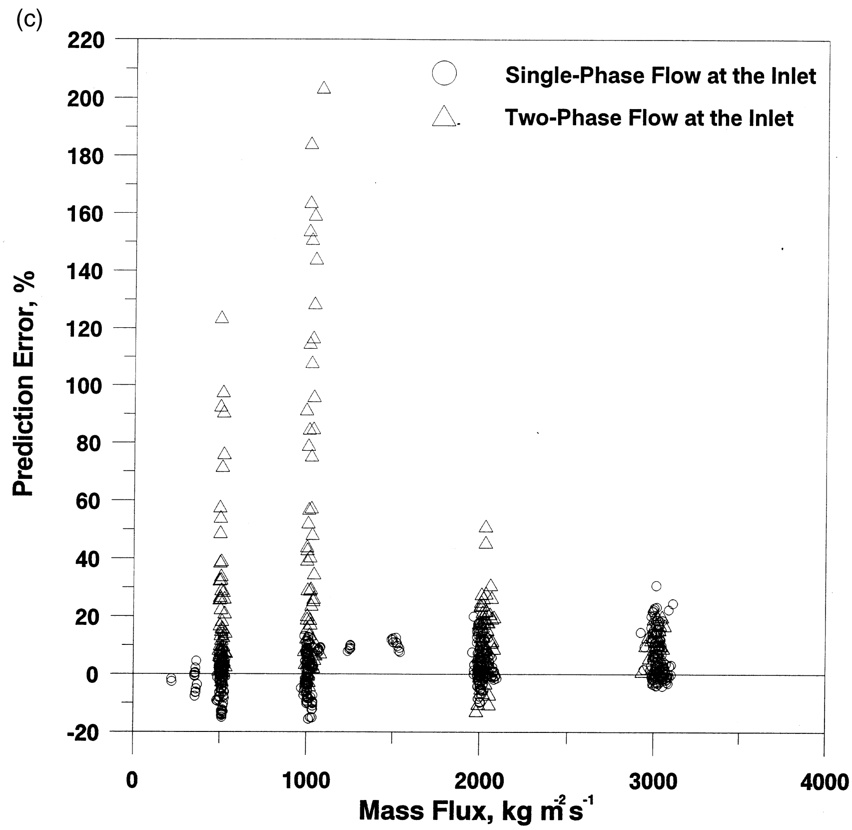

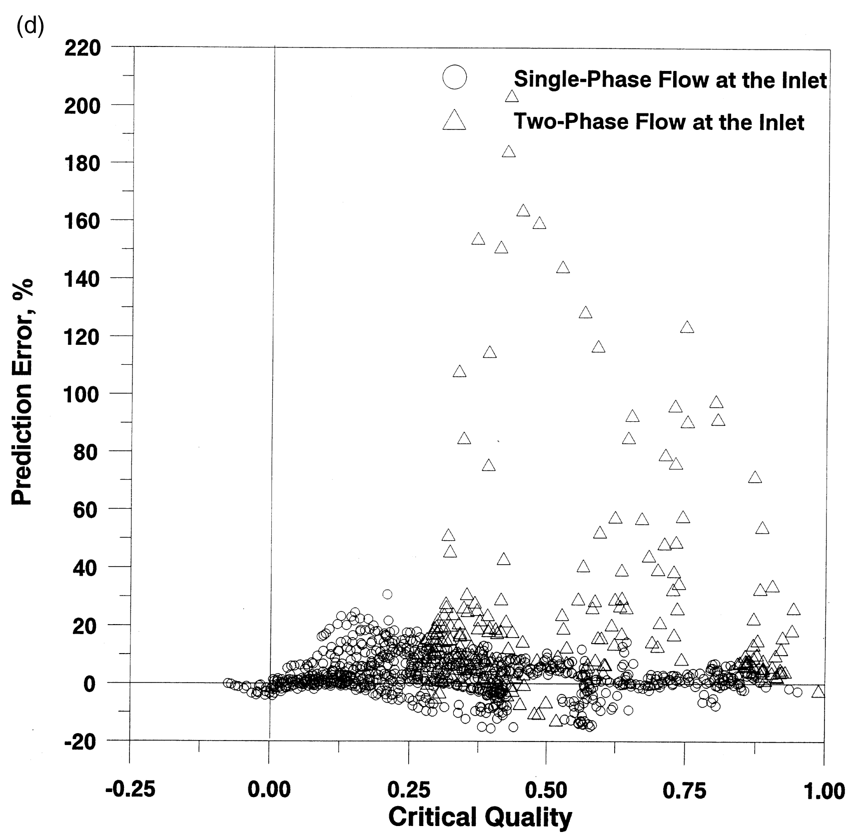

Fig. A1 (*continued*)

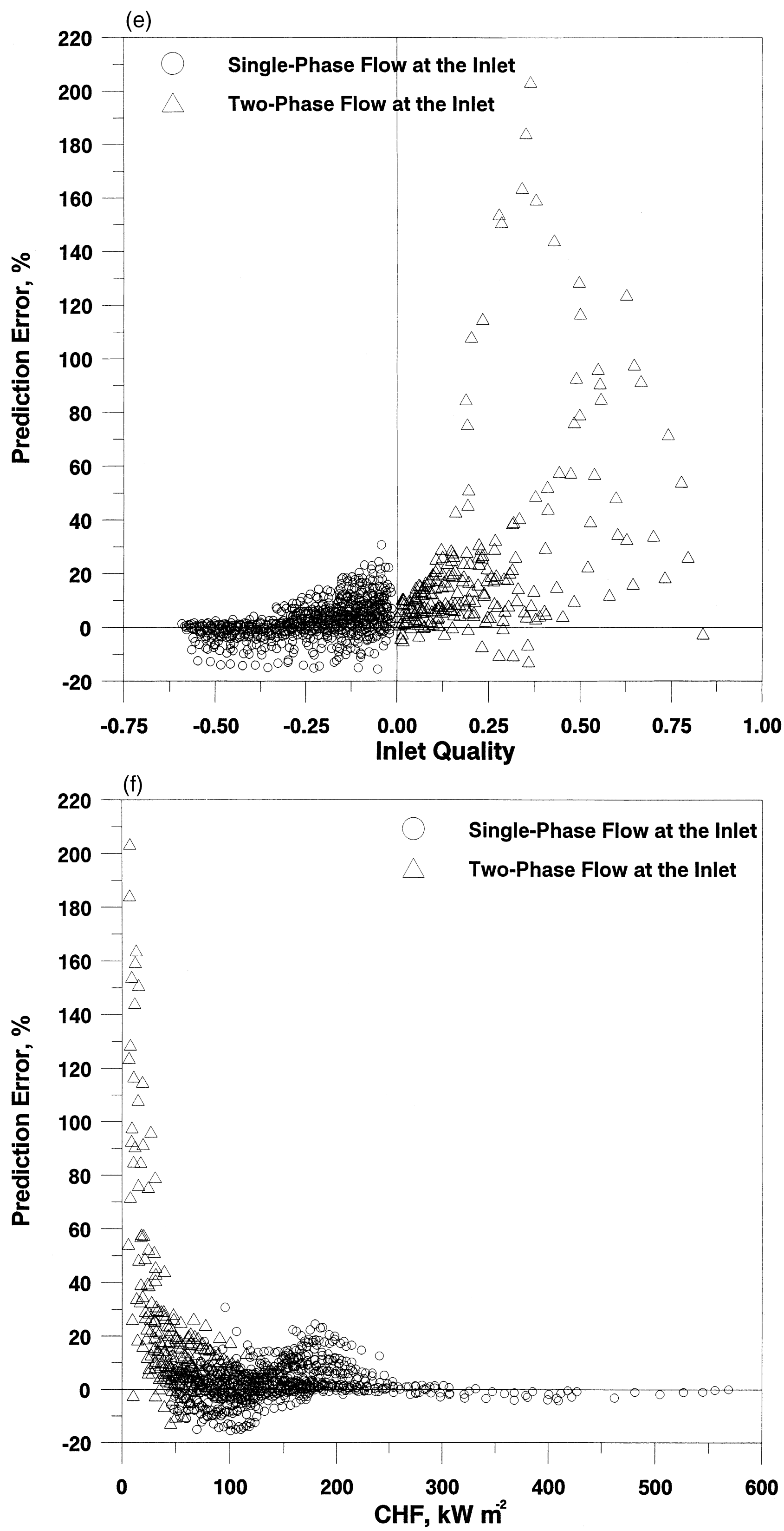

Fig. A1 (*continued*)

References

[1] I.L. Pioro, S.C. Cheng, D.C. Groeneveld, et al., Experimental study of the effect of non-circular flow geometry on the critical heat flux, Nuclear Engineering and Design 187 (1999) 339–362.

[2] I.L. Pioro, S.C. Cheng, A. Vasić, S. Doerffer, Investigation of the effect of non-circular geometry on the critical heat flux under saturated flow boiling conditions, in: Recent Research Developments in Heat, Mass and Momentum Transfer, vol. 2, Research Signpost Publisher, India, 1999, pp. 21–39.

[3] I.L. Pioro, S.C. Cheng, D.C. Groeneveld, et al., Effect of flow obstructions in a circular tube on the critical heat flux (CHF), in: Proceedings of the 17th Canadian Congress of Applied Mechanics (CANCAM'99), Hamilton, Ont., 30 May–3 June, 1999, pp. 267–268.

[4] I.L. Pioro, S.C. Cheng, D.C. Groeneveld, et al., Experimental study of the effect of flow obstructions in a circular tube on the critical heat flux at medium flows, in: Proceedings of the 9th International Topical Meeting on Nuclear Reactor Thermal Hydraulics (NURETH-9), San Francisco, October 3–8, 1999 (Log #227).

[5] D.C. Groeneveld, S. Doerffer, R.M. Tain, et al., Fluid-to-fluid modeling of the critical heat flux and post dry-out heat transfer, in: Proceedings of the World Congress on Experimental Heat Transfer, Fluid Mechanics and Thermodynamics, Brussels, June, vol. 2, 1997, pp. 859–867.

[6] D.C. Groeneveld, D. Blumenrohr, S.C. Cheng, et al., Laboratories using different modeling fluids, in: Proceedings of the 4th International Topical Meeting on Nuclear Thermal Hydraulics (NURETH-4), Salt Lake City, Utah, USA, vol. II, 1992, pp. 531–538.

[7] D.C. Groeneveld, S.C. Cheng, T. Doan, AECL-UO critical heat flux look-up table, Heat Transfer Engineering 7 (1986) 46–62.

[8] R.M. Tain, S.C. Cheng, D.C. Groeneveld, Critical heat flux measurements in a round tube for CFC's and CFC alternatives, International Journal of Heat and Mass Transfer 36 (1993) 2039–2049.

[9] D.C. Groeneveld, L.K.H. Leung, P.L. Kirillov, et al., The 1995 look-up table for critical heat flux in tubes, Nuclear Engineering and Design 163 (1996) 1–23.

[10] V.E. Doroshchuk, L.L. Levitan, F.P. Lantsman, Recommendations for calculating burnout in round tubes, Thermal Engineering 22 (12) (1975) 77–80.

[11] N.M. Galin, P.L. Kirillov, Heat–Mass Transfer in Nuclear Engineering (in Russian), Energoatomizdat, Moscow, 1987, pp. 290–292.

[12] L.S. Tong, Y.S. Tang, Boiling Heat Transfer and Two-Phase Flow, 2nd ed., Taylor & Francis, Bristol, PA, 1997, pp. 369–370.

[13] Recommendations for calculating CHF under water boiling in uniformly heated tubes, Preprint of the Scientific Council for Complex Problem of "Thermal Sciences", Moscow, 1975.

[14] L.L. Levitan, F.P. Lantsman, Investigating burnout with flow of a steam-water mixture in a round tube, Thermal Engineering 22 (1) (1975) 102–105.

[15] V.I. Tolubinskiy, V.A. Antonenko, Yu.N. Ostrovskiy, Boundaries of the region of existence of nucleate boiling surface of saturated liquids, Heat Transfer — Soviet Research 11 (11) (1979) 30–34.

[16] J.B. Kitto Jr., Critical heat flux and the limiting quality phenomenon, AIChE Symposium Ser. Heat Transfer 76 (199) (1980) 57–78.

[17] G.F. Hewitt, Critical heat flux in flow boiling, in: Proceedings of the 6th International Heat Transfer Conference, Toronto, Canada, vol. 6, 1978, pp. 143–171.

[18] I.L. Pioro, S.C. Cheng, A.Ž. Vasić, I. Salah, Experimental evaluation of the limiting critical quality values in circular and non-circular flow geometries, Nuclear Engineering and Design 190 (1999) 317–339.

[19] P. Helzjar, N.E. Todreas, Consideration of critical heat flux margin prediction by subcooled or low quality critical heat flux correlations, Nuclear Engineering and Design 163 (1996) 215–224.